IEEE Access
Multidisciplinary ⋮ Rapid Review ⋮ Open Access Journal

Received 25 July 2025, accepted 6 August 2025, date of publication 15 August 2025, date of current version 28 August 2025.

Digital Object Identifier 10.1109/ACCESS.2025.3599181

RESEARCH ARTICLE

Improving Gait Balance of the Blind During Robot-Assisted Guidance by Providing Static External Reference

JUNYEONG LEE[1], HOSU LEE[2,3], MINKYUNG KIM[1], JIHO PARK[1], AND JUNGWON YOON[1], (Member, IEEE)

[1]Department of AI Convergence, Gwangju Institute of Science and Technology, Gwangju 61005, Republic of Korea
[2]Department of Control and Robot Engineering, Gyeongsang National University, Jinju 52828, Republic of Korea
[3]School of Aerospace Engineering, Gyeongsang National University, Jinju 52828, Republic of Korea

Corresponding author: Jungwon Yoon (jyoon@gist.ac.kr)

This work was supported in part by the Translational Research Center for Rehabilitation Robots under Grant NRCTR-EX23010 and Grant NRCTR-EX24008; in part by the National Rehabilitation Center, Ministry of Health and Welfare, South Korea; in part by the Gwangju Institute of Science and Technology (GIST) Research Institute (GRI) GIST-Cheonnam National University Hospital (CNUH) Research Collaboration grants funded by GIST in 2025; in part by the Culture, Sports and Tourism Research and Development Program through Korea Creative Content Agency grant funded by the Ministry of Culture, Sports and Tourism in 2025 (Project Name: Development of Personalized Exhibition Viewing Concierge Service Technology for the Visually Impaired) under Project RS-2023-00303777, Contribution Rate: 50%; and in part by the Glocal University 30 Project Fund of Gyeongsang National University in 2024 and 2025.

This work involved human subjects or animals in its research. Approval of all ethical and experimental procedures and protocols was granted by the Institutional Review Board of Gwangju Institute of Science and Technology, Gwangju, South Korea, under Application No. 20230919-HR-73-01-01, and performed in line with the Declaration of Helsinki.

ABSTRACT The gait of blind individuals is characterized by reduced gait stability and postural balance due to their limited sensory information. However, existing systems focus on guidance capability rather than improving gait stability and postural balance. Since static external references (SER), such as fixed handrails, can improve the gait balance of the blind, their functionality should be implemented during robot-assisted guidance. In this study, we focused on the proof-of-concept of whether the provision of SER during robot-assisted guidance based on a 3-degrees-of-freedom mobile manipulator, called the robotic haptic cane (RHC), enhances gait stability and postural balance in blind individuals. Accordingly, we conducted gait experiments with 20 blindfolded sighted participants and one blind participant. The experimental results from the blindfolded sighted participants indicate that gait stability (step width variability) and postural balance (mediolateral trunk tilt) are further decreased by walking faster with a blindfold. However, both gait stability and postural balance improved, especially at a faster speed, by using RHC. According to the experimental results of the blind participant, the preferred speed increased with the use of the RHC. In addition, gait stability and postural balance improved with RHC use regardless of speed. Thus, the RHC can enable blind individuals to walk more safely with enhanced gait stability and postural balance by providing SER during robot-assisted guidance.

INDEX TERMS Blind, gait stability, postural balance, robotic haptic cane, static external reference.

I. INTRODUCTION

Worldwide, 285 million people suffer from visual impairment, 39 million of them being blind [1]. Blind individuals tend to adopt a cautious walking strategy characterized by narrowness and slowness since haptic and auditory information should substitute for visual information [2]. Thus, their activities are affected by restricted information due to their disability [3]. They usually use a white cane by tapping to get auditory or haptic information about obstacles or their location on the terrain. Nevertheless, information is limited even with a white cane since the range of information is restricted to the length of the white cane. Accordingly, their pace is slow, even with the use of a white cane [4].

The associate editor coordinating the review of this manuscript and approving it for publication was Yangming Lee.

Visual impairment limits a person's self-motion perception while walking, leading to an unstable gait [5]. Gait in blind individuals is characterized by decreased mediolateral (ML) directional gait stability (step width variability) and postural balance (trunk sway), which is related to falling as well as velocity [5], [6], [7], [8]. Thus, various studies have explored the use of external reference information to augment somatosensory perception, aiming to improve gait stability or postural balance in individuals with impaired vision [5], [6]. Dickstein and Laufer reported that fingertip touch to an external immobile object, serving as a static external reference, can reduce trunk sway in blindfolded individuals while walking on a treadmill [5]. Since haptic information from the handrail provides a spatial reference, it serves as a guide and orientational information, which helps to control ML directional postural oscillation of visually impaired individuals [9]. Furthermore, Kodesh et al. found that walking by touching a fixed handrail (static external reference) rather than a white cane (dynamic external reference) is more helpful in improving step width variability during blindfolded walking [6]. Moreover, since blind individuals better compensate for the lack of vision, they may be better at utilizing haptic information than sighted individuals [10].

Numerous haptic-based systems have been developed to guide the visually impaired. Existing haptic-based guidance systems for the blind use tactile or kinesthetic feedback. Tactile feedback systems utilize directional vibration signals and are worn either on the waist [11] or on the calf [12]. The systems detect surrounding obstacles and guide users with vibration signals, allowing them to avoid obstacles and reach their destination. Since they are wearable, they do not restrict the user's movements. However, the signals are intermittent and require a high level of concentration from the user, and they cannot provide SER to the user. A kinesthetic feedback system that makes contact with the ground to provide continuous and intuitive guidance is designed to be grasped by the user. It includes the robotic white cane system [3], [13], which can move passively in the forward direction by roller and guide direction by a lateral directional actuator at the tip. However, to provide SER, the position of the handle should be controlled in the frontal plane as a rail. Thus, the configuration of the robotic white cane is inadequate to provide SER. There are mobile robot-based systems that mount a handle to navigate the user [14], [15], [16]. However, although the position of the handle can be controlled in the frontal plane, previous mobile robot-based systems are inadequate for providing SER, since the force is inevitably generated at the handle by a torque of the moment arm between the handle and the center of the wheels during the robot's actuation. Moreover, recently, Balatti et al. utilized a mobile manipulator configuration to guide the user by pulling the user with the manipulator when they deviate from the path [17]. However, forcing the user in a lateral direction may impair the user's walking balance. Thus, existing systems have focused on navigation capabilities to improve gait speed rather than gait stability and postural balance. To improve gait stability and postural balance, SER functionality should be implemented in the guidance systems. Meanwhile, although the gait speed of the visually impaired is improved with robotic systems, including robotic white cane and mobile robot-based systems [3], [13], to the best of our knowledge, there is no prior research regarding overground gait analysis of the blind while using such systems although the gait mechanism is changed with faster gait speed [18].

In this paper, our research objective is to improve gait stability and postural balance for blind individuals through haptic information provided as SER implemented by a robotic system. Accordingly, we implemented a 3-DOF mobile manipulator called as RHC system (see Fig. 1 (a)). The configuration of the 1-DOF manipulator driven by a servomotor was added to the 2-DOF mobile robot to provide SER. The configuration of RHC allows the position of the handle to be controlled in the frontal plane as positioned on the path to provide SER while the RHC guides the user along the path (see Fig. 1 (c)). Furthermore, the revolute joint positioned at a fixed angle allows the handle of RHC to be fully stretched (see Fig. 1 (b)), which is a configuration that presents previous mobile robot designs that mount a handle [14], [15]. Accordingly, gait analysis in a straight path was conducted for the proof of concept of the RHC under three conditions: walking without the RHC, using only two actuators of the RHC and the revolute joint is fixed (mobile robot mode), and using all three actuators of the RHC to provide SER (mobile manipulator mode). We hypothesized that the absence of visual information at faster speeds would further decrease gait balance in overground gait. Additionally, we anticipated that providing SER through the RHC would improve gait stability and postural balance, especially at the faster gait speed.

TABLE 1. Abbrevations.

SER	Static External Reference
RHC	Robotic Haptic Cane
PS	Preferred Speed
FS	Fast Speed
RPS	Robot Preferred Speed
EO	Eyes Opened
EC	Eyes Closed
WC	White Cane
MR	Mobile Robot Mode
MM	Mobile Manipulator Mode
ML	Mediolateral
MLD	ML Dominant
MLN	ML Non-Dominant
AP	Anteroposterior
STV	Stride Time Variability
SWV	Step Width Variability

II. METHODS

A. 3 DOF ROBOTIC HAPTIC CANE HARDWARE

The RHC is custom-designed as a simplified mobile manipulator configuration, suitable for investigating gait balance improvement in blind individuals by providing SER.

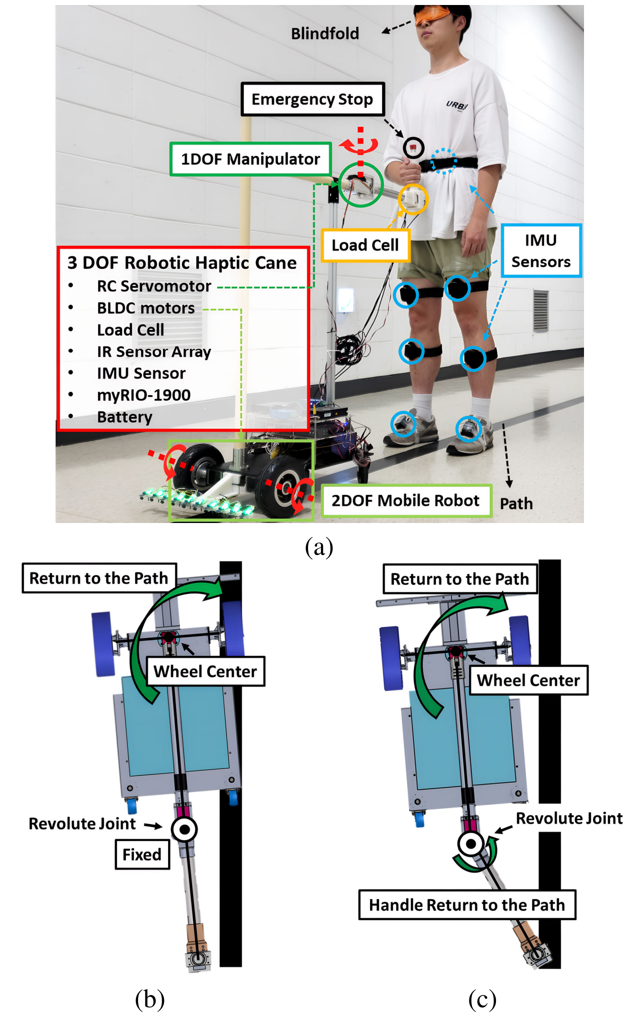

FIGURE 1. **(a) 3 DOF Robotic haptic cane system and an experimental environment. The user wore IMU sensors for gait measurement. In addition, the user held the RHC's handle and walked blindfolded. (b)-(c): Control modes of the robotic haptic cane system for the experiments (b) Mobile robot mode: The position of the wheel center returns to the path when it deviates from the designated path. (c) Mobile manipulator mode: The positions of both the wheel center and the handle return to the designated path.**

TABLE 2. **Specifications of the hardware components.**

Components	Specifications
Battery	22.2V, 13000mAh, ICR30N18650-26-5R-PCM-A Gajinbattery, Republic of Korea
3-axis Load Cell	MS111-200N (Capacity: 200N, Resolution: 0.1N) CASKOREA, Republic of Korea
Amplifier	LCTF, CASKOREA, Republic of Korea
IMU Sensor	BNO055, Bosch Sensortec, German
MCU	myRIO-1900, National Instruments, USA
Motor Driver	Escon 50/5, Maxon, German
BLDC Motor	BG42BL42100E1K, Robotmart, Republic of Korea
RC Servomotor	SAVOX-0236, SAVOX, USA

The components of the RHC are presented in Table 2. The microcontroller unit utilizes the user datagram protocol communication with the laptop over Wi-Fi, where software running in the LabVIEW environment is used to send motor control commands and receive sensor data. As shown in Fig. 1 (a), a 3-axis load cell is mounted on the handle of the RHC to measure the force generated between the user and the RHC. The amplifier amplifies the output signal from the load cell. An inertial measurement unit (IMU) is mounted to measure the robot's yaw angle. It has a built-in sensor fusion algorithm that utilizes an accelerometer, gyroscope, and magnetometer to mitigate sensor noise. It shows low error even during repetitive motion due to its built-in sensor fusion algorithm [19]. The software embedded in the microcontroller unit operates at 200 Hz and generates control signals in the form of an analog voltage for the motor drivers. The motor drivers, in turn, generate motor power for the brushless direct current motors. Motors transfer power through a bevel gear mechanism to the 8 cm radius rigid rubber-driven wheels. Since the position of the handle should be driven according to the set path, the RC servomotor is mounted between the mobile robot part and the handle. A battery powers it and position-controlled within a range of 0-180 degrees at a speed of 47.6 rpm, controlled by a pulse width modulation signal with a frequency of 333 Hz. For safety purposes, a physical stop switch is mounted on the handle, and a software stop is provided on the front panel of the LabVIEW to stop the actuators. The overall system weighs 20 kg, and its maximum speed is 2.39 m/s.

B. CONTROL SCHEME OF THE RHC

Mobile robot systems for the blind guide the user along the path [14], [15]. Therefore, the mobile robot part of RHC should lead the user along the path at a constant speed (see Fig. 1 (b)). Additionally, the system should minimize the path error shown in Fig. 2, which represents the shortest distance between the midpoint of the user's feet and the path. Therefore, the performance of the mobile robot part of RHC can be determined by wheel center error, which is the distance between the center of the RHC wheels and the path. In the previous study [20], the path-following accuracy of a robotic walker to give haptic information was set as a criterion of 20 cm. Likewise, we set the maximum wheel center error as 20 cm to provide guidance over the path with RHC.

As shown in Fig. 3, the wheels of the RHC are controlled based on sensor feedback. Current robotic cane systems utilize sensors such as cameras, LiDAR, infrared sensors, encoders, and IMU [3], [15], [16]. In our framework, we used an infrared sensor array, an IMU, and encoders. Within the infrared sensor array, which is composed of ten infrared sensors, each sensor carries a different weight to determine the robot's position relative to the path. The infrared sensor returns a weight or 0 value depending on whether it passes above the path or not, as e_i shown in Fig. 3. As the robot deviates from the path, the weighted aggregation from the infrared sensor array linearly increases [21]. The IMU is also utilized to measure the yaw angle of the RHC, ensuring smooth movement when deviating from the path. θ_1 is the yaw angle measured by the IMU. The baseline is set at 0 degrees, and a proportional (P) control is applied to the sensor data. After trial and error, the P gain was set at

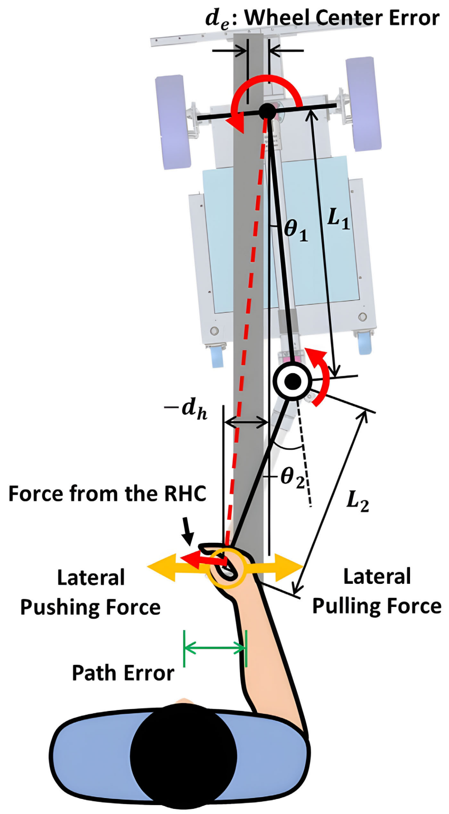

FIGURE 2. Projected view of the robot. (θ_1: yaw angle of the robot, θ_2: angle of the revolute joint, d_e: wheel center error, d_h: position of the handle from the wheel center, L_1, L_2: link parameter of the RHC), Lateral pushing/pulling force is the measured force from the load cell at the handle of the RHC. Path error refers to the distance between the user and the intended path.

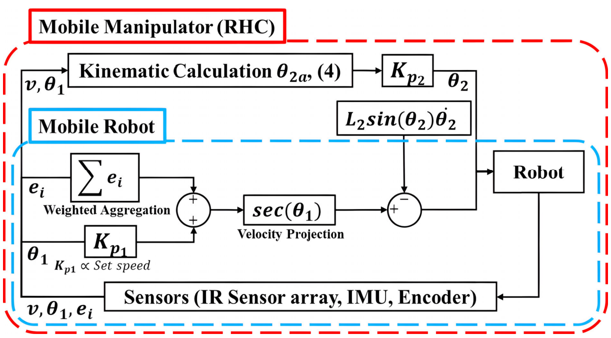

FIGURE 3. Diagram of the control scheme of RHC. The mobile robot is controlled based on feedback from the IMU, encoder, and infrared sensor. The revolute joint controls the position of the handle to follow the path, based on kinematic calculations that utilize encoders and an IMU. (v: average velocity measured from encoders of the wheel-mounted motors, e_i: sensor value of each infrared sensor, θ_1: yaw angle of the robot measured from IMU, θ_2: control command of the actuator on the revolute joint).

0.01 times the preset speed. Therefore, velocity commands for each wheel are adjusted with opposite signs according to the weighted aggregation orientation error, respectively [21]. User safety is considered in situations where the robot fully deviates from the path. When the robot deviates from the path, it only utilizes the IMU, and its heading angle baseline is set to 2.5 degrees to smoothly return to the path. The final velocity command of the robot is then multiplied by $sec(\theta_1)$, to maintain a constant forward speed.

From the previous study [22], the position error of the virtual handrail should be smaller than 6 cm, which is the general human palm width. Therefore, the desired performance of the handle position error is set as 6 cm from the path to provide the SER through the RHC. To achieve this, we utilized an actuator at the revolute joint, enabling it to follow a straight path through kinematic calculations.

$$d_h = L_1 sin(\theta_1) + L_2 sin(\theta_1 + \theta_2) \tag{1}$$

$$d_e = \int_0^T v(t) sin(\theta_1 t) dt \tag{2}$$

$$d_e + d_h = 0 \tag{3}$$

$$\theta_{2a} = -\theta_1 + asin(\frac{-L_1 sin(\theta_1) - d_e}{L_2}) \tag{4}$$

As shown in Fig. 1, the RHC utilizes two independently actuated wheel-based mobile robots and mounts a handle with an additional revolute joint. As shown in Fig. 2, d_h is the lateral position of the robot's handle from the center of the wheels on the plane. d_h is calculated from (1), using kinematic calculation of relative position between the wheel center and the handle, while L_1 and L_2 are the link parameters of the RHC, θ_1 is the yaw angle of the wheel center, and θ_2 is the angle of the revolute joint. As shown in Fig. 2, d_e represents wheel center error, which is the deviation distance of the center of the two wheels from the straight path. d_e is calculated using (2) by integrating the odometry with encoders and an IMU, where v is the average velocity of two wheels, and T is the time from the start of the trial. The sum of the d_h and d_e is the handle position error. The position of the handle should be zero to keep it on the straight path. Therefore, the sum of d_h and d_e should be 0, as indicated in (3). Consequently, (4) is derived from (1)-(3) to ensure that the handle remains on the straight path. In (4), θ_{2a} multiplied by proportional gain K_{p_2} is the control command of the revolute joint of the RHC, which is θ_2. Since the rotational motion direction of the mobile robot and the 1 DOF manipulator is the same (Fig. 2) or different (Fig. 1 (c)), these affect the wheel center error and handle position error differently. Thus, to satisfy the desired wheel center error (d_e, 20 cm) and handle position error ($d_e + d_h$, 6 cm) with various speeds, K_{p_2} was set to 0.5 through trial and error. The wheel center and handle can maintain their position from this equation during the experiments based on the criteria we set.

$$\frac{d}{d\theta_2}(L_1 cos(\theta_1) + L_2 cos(\theta_1 + \theta_2)) = -L_2 sin(\theta_2)\dot{\theta}_2 \tag{5}$$

As shown in Fig. 2, the frontal position of the handle from the center of the wheels projected onto the path is $L_1 cos(\theta_1) + L_2 cos(\theta_1 + \theta_2)$. Accordingly, the position difference due to the θ_2 difference is calculated using (5), which differentiates the frontal position of the handle from the wheel center with respect to the angle of the revolute joint. From (5),

TABLE 3. Experimental protocol.

Sighted Participants	
PSEO	**P**referred **S**peed Gait with **E**yes **O**pened
PSEC	**P**referred **S**peed Gait with **E**yes **C**losed
FSEC	**F**ast **S**peed Gait with **E**yes **C**losed
PSMR	**P**referred **S**peed Gait with **M**oblie **R**obot Mode
PSMM	**P**referred **S**peed Gait with **M**oblie **M**anipulator Mode
FSMR	**F**ast **S**peed Gait with **M**oblie **R**obot Mode
FSMM	**F**ast **S**peed Gait with **M**oblie **M**anipulator Mode
Blind Participant	
PSWC	**P**referred **S**peed Gait with **W**hite **C**ane
FSWC	**F**ast **S**peed Gait with **W**hite **C**ane
PSMR	**P**referred **S**peed Gait with **M**oblie **R**obot Mode
PSMM	**P**referred **S**peed Gait with **M**oblie **M**anipulator Mode
FSMR	**F**ast **S**peed Gait with **M**oblie **R**obot Mode
FSMM	**F**ast **S**peed Gait with **M**oblie **M**anipulator Mode
RPSMR	**R**obot **P**referred **S**peed Gait with **M**oblie **R**obot Mode
RPSMM	**R**obot **P**referred **S**peed Gait with **M**oblie **M**anipulator Mode

the position difference due to the θ_2 difference is $-L_2 sin(\theta_2)\dot{\theta}_2$, and it is added to the mobile robot part's final velocity command.

III. EXPERIMENT

We conducted a straight path gait experiment to evaluate the effect of the developed system. 20 sighted participants (10 males, 10 females, Age: 22.0 ± 2.3 years, Height: 168.6 ± 7.5 cm, Weight: 63.7 ± 13.9 kg, Dominant Side: Right 17, Left 3) and 1 blind participant (Male, Age: 47, Height: 170.1 cm, Weight: 70.5 kg, Dominant Side: Right, Congenitally blind) took part in the experiment. The study included volunteers who reported no vestibular disorders and had no difficulty using the RHC. The experiment was conducted in accordance with the Declaration of Helsinki and was approved by the Institutional Review Board of Gwangju Institute of Science and Technology, Gwangju, South Korea (20230919-HR-73-01-01). Prior to the experiment, all participants provided written or oral informed consent. The participants were verbally introduced to the RHC's role and how to use it. The participants conducted gait experiments under the conditions shown in Table 3. Two trials were conducted under each condition.

A. EXPERIMENT: SIGHTED PARTICIPANTS

Sighted participants were blindfolded to simulate blindness, except in the PSEO condition. In the PSEO trials, participants were instructed to walk along the path shown in Fig. 1 (a) at their preferred speed. In the PSEC trials, participants were asked to walk at their preferred speed while attempting to follow the path, considering their postural orientation during the trial. Similarly, in the FSEC trials, participants were instructed to walk at a voluntary fast speed while also trying to follow a straight path, considering their orientation.

During experiments involving the robot (MR and MM), the participants were required to grip the RHC's handle. As shown in Fig. 1 (b), for the MR, the revolute joint of RHC was fixed to make the handle of RHC fully stretched. In PSMR and PSMM conditions, the robot's speed was determined based on the speed of PSEC. Likewise, in the FSMR and FSMM conditions, the robot's speed was based on the speed of FSEC. Since the baseline speed of the robot needed to be established first, the experimental procedure was pseudo-randomized, beginning with the EC condition, followed by randomly assigned MR and MM conditions. The total experimental time was 45 minutes for the sighted participant, and a 3-minute rest was given between protocols.

B. EXPERIMENT: THE BLIND PARTICIPANT

Based on the results of the sighted participants, a pilot experiment was conducted with a blind participant. Since blind individuals are generally trained to use assistive devices such as white canes, we included WC trials as a baseline. For the trials, a blind participant was given 10-m-long Braille blocks, which were placed so that the user could walk by detecting the path with a white cane during the WC trials.

The robot speed of the PSMR and PSMM trials was determined based on the speed observed in the PSWC trials. Likewise, in the FSMR and FSMM conditions, the robot's speed was based on the speed of FSWC trials. The experiment was also pseudo-randomized, beginning with the WC condition, followed by randomly assigned MR and MM conditions. The total experimental time was 1 hour, and a 3-minute rest was given between protocols. In addition, since RHC can improve the gait balance of sighted participants during fast speed trials (Section IV-A), the preferred speed when using the robot should also be investigated. Accordingly, we gradually increased the speed of the robot in the PSMM to determine the preferred speed when using the robot (RPS), which was set as the speed of the robot for the RPSMR and RPSMM trials [8]. For the MR and MM trials, the participant walked along a 12 m straight path.

C. DATA COLLECTION AND ANALYSIS

As shown in Fig. 1 (a), participants wore an IMU (Myomotion, Noraxon, USA) on their pelvis, shanks, thighs, and feet to collect kinematic gait data. Data recorded during the middle 10 m of a 12 m section were used for analysis, and data from 8 m of a 10 m section were used for analyzing WC trials. The starting and ending points of the 10 m segment were marked during the experiments using the internal software of the gait measurement sensor [23].

RHC's velocity, wheel center, and handle position error were measured using encoders and an onboard IMU. Additionally, force data were measured using the handle-mounted load cell. Velocity, error, and force were recorded using software running in the LabVIEW environment at a sampling rate of 200 Hz. Gait speed was measured using a stopwatch. As shown in Fig. 2, the path error at the arrival point, which represents the shortest distance between the path and the middle of the participant's feet, was measured using a tape measure, and the path errors below 1 cm were ignored. The IMU data were processed using the MR3 (Noraxon, USA) software to obtain the mediolateral (ML)

TABLE 4. Overall experimental results.

Sighted Participants							
Parameter	**PSEO**	**PSEC**	**FSEC**	**PSMR**	**PSMM**	**FSMR**	**FSMM**
Velocity (m/s)	1.23±0.25	0.83±0.19	1.27±0.36	0.77±0.19	0.77±0.19	1.25±0.41	1.25±0.42
Path Error (cm)	0.00±0.00	43.15±24.80	41.18±28.37	9.03±3.93	9.53±5.02	8.56±4.69	8.58±6.55
RMS of ML (degree)	1.81±0.65	1.69±0.42	1.99±0.52	1.49±0.43	1.61±0.35	1.73±0.48	1.82±0.43
RMS of AP (degree)	3.12±1.74	3.60±1.57	4.32±2.54	3.58±2.32	3.49±2.15	3.47±1.93	3.35±1.93
RMS of MLD (degree)	1.50±0.79	1.35±0.66	1.63±0.74	1.22±0.52	1.26±0.59	1.64±0.65	1.31±0.66
RMS of MLN (degree)	1.61±0.66	1.43±0.64	1.65±0.69	1.39±0.60	1.38±0.56	1.35±0.54	1.70±0.64
Lateral Pushing Force (N)	-	-	-	0.46±0.24	0.46±0.25	0.42±0.16	0.61±0.32
Lateral Pulling Force (N)	-	-	-	0.37±0.20	0.41±0.16	0.53±0.22	0.42±0.18
STV (ms)	25.68±6.76	59.91±22.17	44.63±17.41	47.58±18.85	35.95±11.37	34.36±11.96	30.89±9.58
SWV (mm)	15.97±4.15	30.45±10.06	39.44±15.01	28.98±14.29	24.29±8.18	35.09±15.65	26.07±8.33

Blind Participant								
Parameter	**PSWC**	**FSWC**	**PSMR**	**PSMM**	**FSMR**	**FSMM**	**RPSMR**	**RPSMM**
Velocity (m/s)	1.06±0.09	1.41±0.67	1.02±0.00	1.01±0.01	1.36±0.04	1.40±0.01	1.42±0.03	1.34±0.04
Path Error (cm)	0.00±0.00	0.25±0.25	24.80±3.40	3.55±3.55	9.55±1.55	11.90±8.50	17.80±7.60	14.90±3.40
RMS of ML (degree)	1.68±0.09	1.85±0.08	1.31±0.12	1.06±0.04	2.23±0.89	1.16±0.17	1.78±0.43	1.29±0.38
RMS of AP (degree)	4.63±0.44	7.30±1.00	4.09±0.21	3.50±0.28	4.44±2.37	4.45±1.81	6.20±2.42	4.85±0.35
RMS of MLD (degree)	1.38±0.45	2.15±0.15	1.32±0.15	1.13±0.04	2.27±0.81	0.93±0.47	1.78±0.41	1.15±0.45
RMS of MLN (degree)	1.30±0.74	2.08±0.03	1.42±0.19	1.25±0.11	1.63±0.91	2.03±0.86	1.89±1.41	2.22±1.33
Lateral Pushing Force (N)	-	-	1.04±0.27	1.15±0.04	1.09±0.04	1.81±0.70	0.96±0.59	1.75±0.47
Lateral Pulling Force (N)	-	-	1.06±0.39	1.04±0.55	1.47±0.20	1.03±0.12	1.37±0.62	0.86±0.05
STV (ms)	77.66±22.99	50.29±7.79	36.24±6.45	36.18±10.87	36.08±10.80	17.58±2.09	24.99±2.67	22.87±4.80
SWV (mm)	63.68±28.92	64.49±18.07	67.34±11.43	21.30±3.53	76.87±10.32	35.15±3.78	72.33±3.41	26.99±3.45

and anteroposterior (AP) pelvic tilts, stride time variability (STV) [24], and step width variability (SWV) [6]. Pelvic tilt implies postural balance; STV and SWV are the gait stability parameters. Higher values imply poor balance and unstable gait, respectively [6], [8], [24]. To calculate SWV, the standard deviation of the step width measured during the initial contact phase of both feet was used [6]. Lateral force data were measured to investigate how the SER of the RHC affects the user's balance directionally. The sum of the measured forces in the two axes of the transverse plane was projected in the vertical direction along the path for data analysis. As shown in Fig. 2, lateral force data were processed directionally, with pushing/pulling indicating the force in the direction inside/outside from the user's dominant hand. Positive lateral force indicates the pulling direction. ML pelvic tilt data are also processed directionally as ML Dominant and ML Non-dominant. ML Dominant indicates the direction of the hand holding the handle of the RHC. A purpose-built software running in the MATLAB environment was used to calculate the RMS of ML (ML Dominant & Non-dominant) & AP, lateral pushing/pulling force, and SWV.

A 1-way repeated-measures analysis of variance (RMANOVA) was used to analyze the differences between PSEO, PSEC, and FSEC in velocity, path error, RMS of ML & AP of trunk tilt angle, STV, and SWV. 2-way RMANOVA was used to investigate the differences due to Speed (PS, FS) and Condition (EC, MR, MM) in velocity, path error, RMS of ML (Dominant, Non-dominant) & AP of trunk tilt angle, STV, and SWV. To analyze the differences in Speed (PS, FS) and Condition (MR, MM) for lateral forces, a 2-way RMANOVA was used. The Q-Q plot evaluation tool was used to assess the normality of the data distribution. To confirm the validity of the RMANOVA results, Mauchly's test of Sphericity was used, and Greenhouse-Geisser corrections were applied where sphericity was violated. Post-hoc tests were performed using the Bonferroni correction. Analysis was conducted with SPSS V20.0 (IBM Corp., USA).

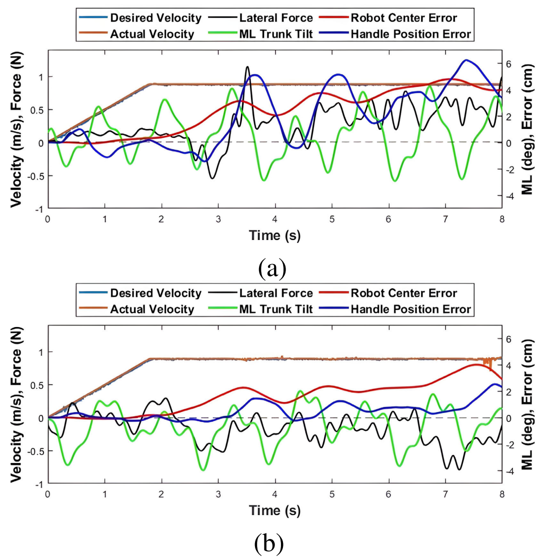

FIGURE 4. Device data (velocity, wheel center & handle position error), lateral force data, and ML trunk tilt data during a representative experiment trial. (a) Mobile Robot mode trial (b) Mobile Manipulator mode trial for Fast Speed. Positive lateral force indicates the direction of the lateral pulling force (Outside direction of the user's dominant hand).

IV. RESULT & DISCUSSION

Overall experimental results are presented in Table 4. In addition, the results of statistical analyses are presented in Table 5.

TABLE 5. Results of the statistical analyses.

Parameter	Factor	F	P-value	η_p^2
1-way RMANOVA				
Velocity	-	(2,38)=38.42	**< .001**	**.669**
Path Error	-	(1.364,25.920)=18.517	**< .001**	**.494**
RMS of ML	-	(2,38)=4.91	**< .05**	**.205**
RMS of AP	-	(1.342,25.494)=2.355	.130	.110
STV	-	(2,38)=27.925	**< .001**	**.595**
SWV	-	(2,38)=30.839	**< .001**	**.619**
2-way RMANOVA				
Velocity	Speed	(1,19)=42.253	**< .001**	**.690**
	Condition	(1.255,23.851)=2.004	.168	.095
	Interaction	(2,38)=.743	.482	.038
Path Error	Speed	(1,19)=.114	.730	.006
	Condition	(1.099,20.886)=57.840	**< .001**	**.753**
	Interaction	(1.030,19.561)=.263	.620	.014
RMS of ML	Speed	(1,19)=19.139	**< .001**	**.502**
	Condition	(2,38)=7.223	**< .01**	**.275**
	Interaction	(2,38)=.558	.577	.029
RMS of AP	Speed	(1,19)=.231	.636	.012
	Condition	(1.371,26.046)=1.187	.304	.059
	Interaction	(1.434,27.255)=1.262	.288	.062
RMS of MLD	Speed	(1,19)=11.819	**< .01**	**.384**
	Condition	(1.535,29.161)=4.245	**< .05**	**.183**
	Interaction	(1.394,26.479)=4.183	**< .05**	**.180**
RMS of MLN	Speed	(1,19)=11.159	**< .01**	**.370**
	Condition	(1.477,28.060)=3.648	.051	.161
	Interaction	(2,38)=5.094	**< .05**	**.211**
Lateral Pushing Force	Speed	(1,19)=3.519	.076	.156
	Condition	(1,19)=7.233	**< .05**	**.276**
	Interaction	(1,19)=11.972	**< .01**	**.387**
Lateral Pulling Force	Speed	(1,19)=18.075	**< .001**	**.488**
	Condition	(1,19)=1.179	.291	.058
	Interaction	(1,19)=13.541	**< .01**	**.416**
STV	Speed	(1,19)=18.489	**< .001**	**.493**
	Condition	(1.410,26.795)=22.484	**< .001**	**.542**
	Interaction	(1.372,26.070)=2.559	.112	.119
SWV	Speed	(1,19)=4.483	**< .05**	**.191**
	Condition	(2,38)=11.363	**< .001**	**.374**
	Interaction	(1.351,25.670)=1.786	.194	.086

A. SIGHTED PARTICIPANTS

Velocity, wheel center, handle position errors of RHC, lateral force, and ML trunk tilt of representative trials are shown in Fig. 4. Results of the 1-way RMANOVA are presented in Fig. 5. Results of the 2-way RMANOVA for velocity, path error, RMS of ML, STV, SWV, RMS of ML Dominant, and Non-dominant are presented in Fig. 6. There was no significant interaction between Speed and Condition for velocity, path error, RMS of ML, RMS of AP, STV, and SWV, which led to separate post-hoc analysis. There was no significance in the RMS of AP. The 2-way RMANOVA results for the lateral forces are presented in Fig. 7.

As shown in Fig. 5 (a), the velocity under PSEC showed a significant reduction compared to PSEO and FSEC (P<.001 for PSEO vs PSEC, Cohen's D: 1.826, P<.001 for PSEC vs FSEC, Cohen's D: 1.506). However, there was no significant difference between the velocities of PSEO and FSEC. These findings indicate that gait velocity decreases when walking blindfolded, which is consistent with a previous study [6]. Nevertheless, gait velocity can be restored to a sighted condition by walking at a voluntary fast speed while blindfolded. SWV under EC trials significantly increased compared to PSEO (P<.001 for PSEO vs PSEC, Cohen's D: 1.881, P<.001 for PSEO vs FSEC, Cohen's D: 2.132). Additionally, while the velocities of the PSEO and FSEC did not show significant differences, the STV increased significantly (P<.05 for PSEO vs FSEC, Cohen's D: 1.435). Since STV is affected by gait velocity [24], these results indicate that the blindfolded condition disturbed the gait. Furthermore, there were significant differences in the RMS of ML (see Fig. 5 (c), P<.001 for PSEC vs FSEC, Cohen's D: 0.635) and SWV (see Fig. 5 (e), P<.05 for PSEC vs FSEC, Cohen's D: 0.704) between PSEC and FSEC. Thus, the participants experienced disturbances in ML-directional gait stability and postural balance with voluntary fast speed compared to preferred speed [6], [8]. Therefore, as our hypothesis, the gait balance of the blindfolded participants was further disturbed when walking at a voluntary fast speed compared to the preferred speed.

As shown in Fig. 6 (a), in both speed trials in path error, a significant difference was found between EC and MR, EC and MM (P<.001 for PSEC vs PSMR, Cohen's D: 1.922, P<.001 for PSEC vs PSMM, Cohen's D: 1.879, P<.01 for FSEC vs FSMR, Cohen's D: 1.604, P<.001 for FSEC vs FSMR, Cohen's D: 1.583). This indicates that RHC can guide the user along the path. However, since there was no significant difference between MR and MM in velocity and path error, the mode may not impact the guidance functionality of the RHC. Therefore, using RHC can guide users as previous robotic systems have [14], [15].

As shown in Fig. 6 (c), in PS trials of STV, a significant difference was found between each of PSEC and PSMR compared to PSMM (P<.001 for PSEC vs PSMM, Cohen's D: 1.360, P<.01 for PSMR vs PSMM, Cohen's D: 0.747). Also, in FS trials in STV, a significant difference was found between each of FSMR and FSMM vs FSEC (P<.01 for FSEC vs FSMR, Cohen's D: 0.688, P<.01 for FSEC vs FSMM, Cohen's D: 0.978). Wuehr et al. reported that sensory feedback contributes more during slow locomotion; however, passive biomechanical mechanisms and automated central pattern generator control gait during fast locomotion on the treadmill without visual information [7]. Therefore, STV at the preferred speed may be reduced by the SER from the RHC-provided sensory feedback. On the other hand, STV under the FS condition may be reduced regardless of the mode due to the central pattern generator contributing more at the gait velocity regulated to a fast speed.

In all three conditions, the RMS of ML showed a significant difference between PS and FS (see Fig. 6 (h), P<.01 for PSEC vs FSEC, Cohen's D: 0.635, P<.01 for PSMR vs FSMR, Cohen's D: 0.528, P<.01 for PSMM vs FSMM, Cohen's D: 0.552). Thus, walking at a voluntary fast speed affects the ML trunk sway under blindfolded conditions. In addition, as shown in Fig. 6 (b), the RMS of ML trunk tilt at MR under FS was significantly reduced compared to EC (P<.05 for FSEC vs FSMR, Cohen's D: 0.517). Afzal et al. reported that kinesthetic haptic feedback based on a mobile robot reduces trunk sway [25]. There is no significant difference between EC and MM under FS (see Fig. 6 (d)). However, as shown in Fig. 6 (e),

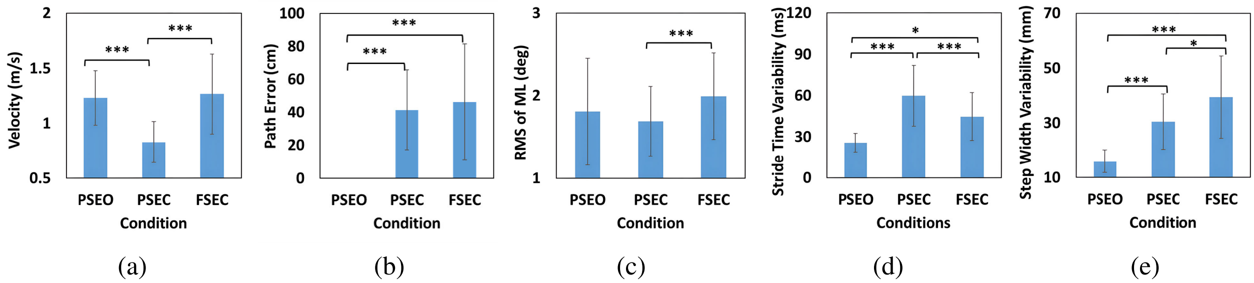

FIGURE 5. 1-way RMANOVA results for the gait experiment with sighted participants for conditions without robot: Preferred Speed with Eyes-Opened, Preferred speed with Eyes-Closed, and Fast speed with Eyes-Closed, (a) Velocity, (b) Path error, (c) RMS of ML, (d) Stride time variability, and (e) Step width variability The colored bars show the mean and the error bars show the standard deviation. Statistically significant differences are marked based on the Post-hoc pairwise comparisons (*: P<.05, **: P<.01, and ***: P<.001.)

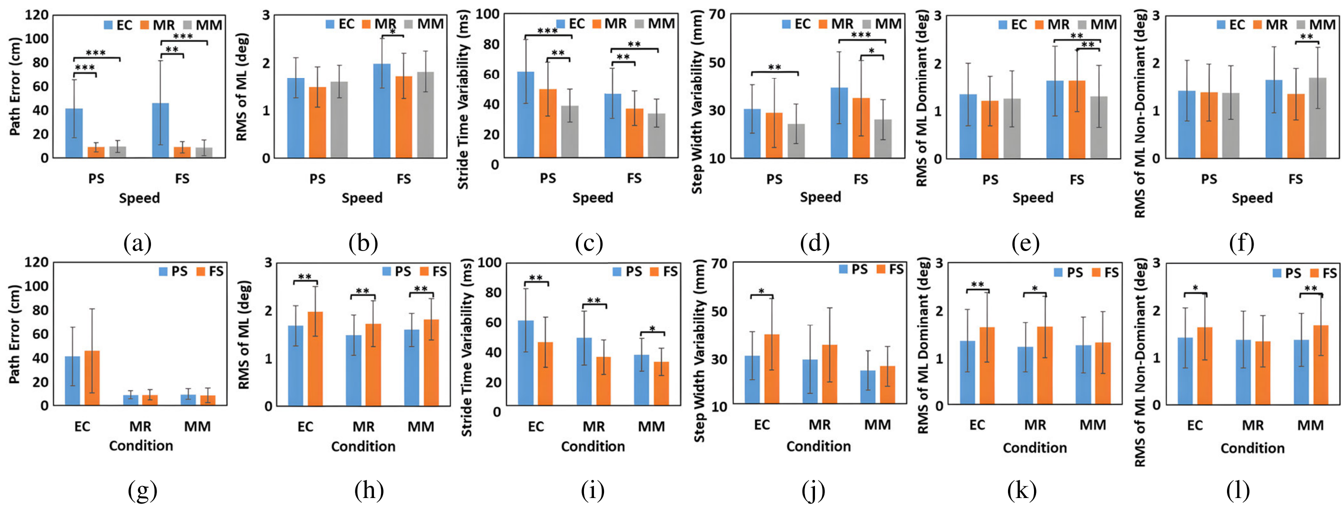

FIGURE 6. 2-way RMANOVA results for the gait experiment with sighted participants: (a)-(f) compare for guidance condition (Eyes Closed, Mobile Robot mode, Moblie Manipulator mode), (g)-(l) speed (Preferred Speed, Fast Speed), (a): Path error for condition, (b): RMS of ML for condition, (c): Stride time variability for condition, (d): Step width variability for condition, (e): RMS of ML dominant for condition, (f): RMS of ML non-dominant for condition, (g): Path error for speed, (h): RMS of ML for speed, (i): Stride time variability for speed, (j): Step width variability for speed, (k): RMS of ML dominant for speed, and (l) RMS of ML non-dominant for speed. The colored bars show the mean, and the error bars show the standard deviation. Statistically significant differences are marked based on the Post-hoc pairwise comparisons (*: P<.05, **: P<.01, and ***: P<.001.)

the RMS of ML Dominant of trunk tilt at MM under FS condition was significantly reduced compared to EC and MR (P<.01 for FSEC vs FSMM, Cohen's D: 0.459, P<.01 for FSMR vs FSMM, Cohen's D: 0.500). Furthermore, the lateral pushing force was significantly higher (see Fig. 7 (a), P<.01 for FSMR vs FSMM, Cohen's D: 0.754), and the lateral pulling force was lower (see Fig. 7 (c), P<.01 for FSMR vs FSMM, Cohen's D: 0.512) at MM than at MR under FS. These results demonstrated that the ML trunk sway in the direction of the dominant hand may be reduced by the lateral pushing force, which is in the opposite direction of ML trunk sway. The handle of the RHC served as a fixed object providing orientation reference, thereby affecting the improvement of balance in the dominant hand direction with haptic supplementation [9]. Furthermore, Jeka et al. reported that since the amount of lateral force is the same as trunk sway in the opposite direction while using a slanted cane, it reduces trunk sway more than a vertical cane [26]. Therefore, the RHC may improve balance by providing orientation reference and opposite directional force in the direction of trunk sway.

As shown in Fig. 6 (j), only in the EC trials of SWV, there was a significant difference between PS and FS (P<.05 for PSEC vs FSEC, Cohen's D: 0.704). Since there is no significant difference between PS and FS in the MR and MM conditions, ML-directional gait stability did not decrease with faster speed trials when using RHC. In PS trials of SWV, as shown in Fig. 6 (d), a significant difference was observed between PSEC and PSMM (P<.01 for PSEC vs PSMM, Cohen's D: 0.672). In FS trials of SWV, significant differences were found between FSEC and FSMR vs FSMM (P<.001 for FSEC vs FSMM, Cohen's D: 1.102, P<.05 for FSMR vs FSMM, Cohen's D: 0.720). Kodesh et al. reported that SWV is reduced by touching the handrail (SER) to the blindfolded, while it is not reduced when walking with the white cane (dynamic external reference) [6]. Since only the MM showed a significant decrease in the SWV at both speeds, ML gait stability can be improved with the developed RHC. Additionally, in the MR, the position of the handle moves in sync with the mobile robot part, so the handle position also moves accordingly (see Fig. 4 (a)). Thus, gait stability may not be improved with MR. SWV

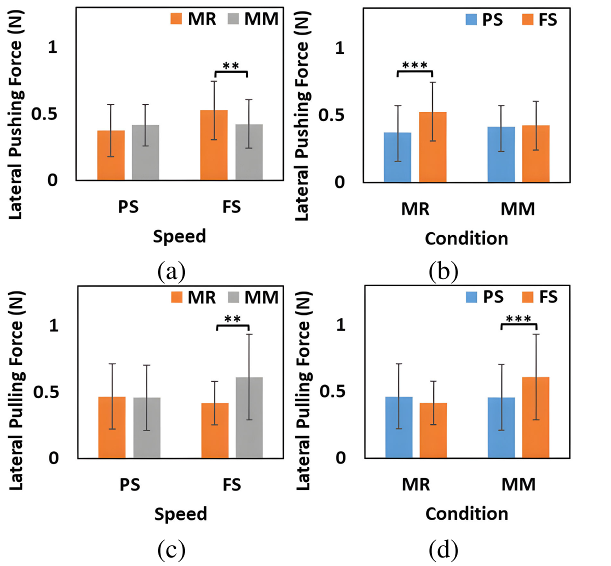

FIGURE 7. 2-way RMANOVA results for the measured lateral force with direction: (a), (c) compare for guidance condition (Mobile Robot mode, Moblie Manipulator mode), (b), (d) speed (Preferred Speed, Fast Speed) (a): Lateral pushing force for condition, (b): Lateral pushing force for speed, (c): Lateral pulling force for condition, (d): Lateral pulling force for speed. The colored bars show the mean, and the error bars show the standard deviation. Statistically significant differences are marked based on the Post-hoc pairwise comparisons (*: P<.05, **: P<.01, and ***: P<.001.)

is the indicator of the ML plane gait stability and is a more meaningful descriptor of gait control compared to other variability parameters [6], [27]. Therefore, the RHC can enhance the gait stability of the blindfolded participants by providing an SER.

B. THE BLIND PARTICIPANT

A pilot test was conducted on a blind participant, based on the results of experiments with blindfolded participants, to investigate the potential of the SER for improving gait balance compared to the conventional device typically used by the blind. The results are presented in Fig. 8. Since blindfolded participants exhibited improved gait balance while walking with the RHC during FS trials, using the RHC may enhance the preferred speed of the user. Thus, we included the RPS conditions in the pilot experiment for a blind participant. As shown in Fig. 8 (a), the preferred speed improved to the same level as the velocity measured in FS trials while using the RHC (FS: 1.41 m/s, RPS: 1.42 m/s). Similarly, gait performance measured during RPS trials exhibited the same trends as those observed during FS trials (see Table 4). The participant commented that he could walk faster since he had confidence in using the RHC, which could guide him directly along the designated path. Haibach et al. reported that visually impaired individuals with lower confidence intentionally reduced participation in physical activity [28]. Therefore, navigation systems, including RHC, may improve blind users' gait velocity by enhancing confidence.

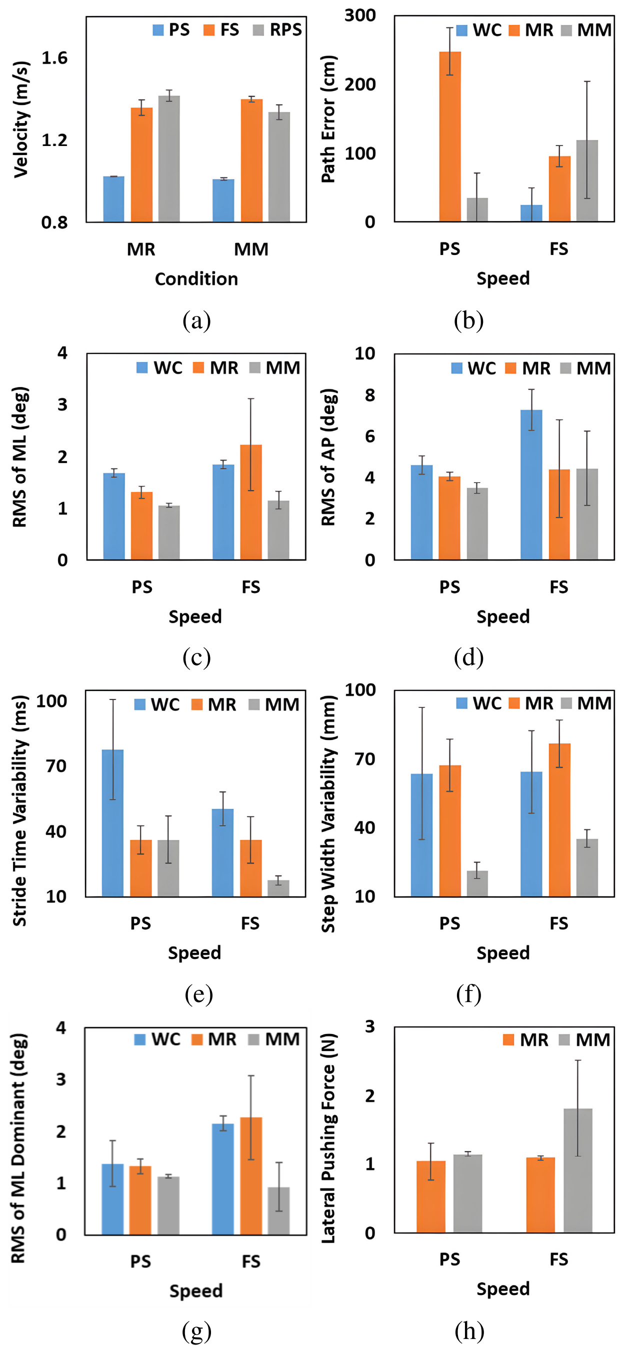

FIGURE 8. Experimental results with a blind participant: (a) velocity, (b) path error, (c) RMS of ML, (d) RMS of AP, (e) Stride time variability, (f) Step width variability, (g) RMS of ML Dominant, (h) RMS of ML Non-dominant. The colored bars show the mean and the error bars show the standard deviation.

As shown in Fig. 8 (b), the path error showed different trends compared to the results of sighted participants. For trials using the RHC, the standard deviation was high compared to WC trials. Visually impaired people are accustomed to using Braille blocks and white canes, however, the participant was relatively less accustomed to using the RHC. Furthermore, WC trials showed lower path error regardless of gait velocity. In trials using the WC, information about path errors was transmitted from the Braille blocks as the participant walked while pushing the cane along the straight pattern of the Braille blocks. Thus, the deviation may be higher in the RHC trials, and the path error may be smaller with a white cane. Therefore, it may become necessary to be accustomed to the RHC to walk with a low path error.

STV was higher in the WC trials compared to trials with the RHC (see Fig. 8 (e)). In addition, Moon et al. reported that AP postural balance is correlated with STV [29]. In the case of the blind participant, the RMS of AP also decreased in RHC trials compared to WC trials (see Fig. 8 (d)). The RMS of AP may show different trends from those of sighted participants since the blind participants used the white cane trials as their baseline. The tip of the white cane can get caught in the unevenness between the straight-arranged Braille blocks, as the user slides the white cane over the Braille block [30]. Thus, STV and RMS of AP may be higher in WC trials. Additionally, similar to the results of sighted participants, the STV in the blind participant may be improved through sensory feedback and velocity regulation via RHC [7]. Thus, the blind participant may have improved gait balance in the AP direction by the RHC.

ML gait stability (SWV) and postural balance (RMS of ML) showed different results compared to sighted participants. In the blind participant, gait stability and postural balance were not improved in MR mode; however, they were enhanced in MM mode regardless of speed. The participant reported psychological security during MM trials. Balance, as well as velocity, was associated with confidence in visually impaired individuals [28]. The SER provided through the MM mode may have improved confidence by offering the lateral force required by the user, whereas the MR mode could not provide an SER to the user. As in the case of sighted participants, the balance of the blind participant improved since the lateral force (pushing) in the dominant direction might compensate for the balance in that direction (see Fig. 8 (g) and (h)). Since blind individuals better compensate for the lack of vision, MM was effective regardless of speed, different from the sighted participants [10]. Therefore, it is necessary to provide a SER through the MM mode of the RHC for the visually impaired.

C. FINDINGS AND FUTURE WORKS

The results of sighted participants imply that walking with a blindfold at a faster speed further disturbs gait balance. Although a faster speed can reduce STV (Fig. 5 (d)), ML postural balance (RMS of ML, Fig. 5 (c)) and gait stability (SWV, Fig. 5 (e)) remain disturbed. However, the postural balance (RMS of ML Dominant, Fig. 6 (e)) is improved by the SER provided by the RHC at the faster speed. In addition, gait stability (SWV, Fig. 6 (d)) is enhanced by the lateral pulling force (Fig. 7 (c)) from the RHC at both preferred and fast speeds.

The results of the blind participant showed different trends from those of the sighted participants. Since the baseline condition was the white cane trial, which is familiar to the blind user, navigation performance (path error (Fig. 8 (b))) may be higher than that with RHC. In addition, they actively use non-visual sensory input to adapt to the environment [31]. Since long-term lack of vision results in improved management of haptic information [10], both gait stability (SWV, Fig. 8 (f)) and postural balance (RMS of ML, Fig. 8 (g)) may be improved compared to white cane trials, regardless of speed. Since the handle of the white cane is not fixed stably on the path as a rail, even if it provides grounded information, it corresponds to a dynamic external reference. However, the position of the handle of the RHC can be controlled in the frontal plane as a rail, which can provide a static external reference. Therefore, the developed RHC has the potential to improve the gait balance of the blind. However, since this study includes a limited number of blind participants, a better understanding of the balance strategy of blind individuals requires experimental analysis with a larger number of blind participants and various age distributions.

Conclusively, we investigated the improvement of gait stability and postural balance through the developed RHC system at different gait speeds on a straight path with blindfolded sighted participants and a blind participant. Our research purpose was to provide proof-of-concept for the SER functionality during the robot-assisted guidance with the RHC system on the gait balance of the blind. Although the pilot test confirmed the potential of SER provided by robots, it is difficult to generalize the experimental results since only one visually impaired participant participated in the experiment. For example, experimental results in FSMM trials, especially with high deviation within trials (i.e., path error (Fig. 8 (b)), RMS of AP (Fig. 8 (d)), and RMS of ML dominant (Fig. 8 (g))), may show different results due to individual variety. Accordingly, experimental verification with a large number of patients with various visually impaired cohorts, such as low vision and congenital or acquired blindness, is necessary as future work. In addition, although we included the WC and RS trials, a comparison with other existing robotic systems (e.g., robotic white canes) is also necessary to demonstrate the effectiveness of our system more clearly. We found that the SER enhanced gait balance since the RHC can control the handle position in the frontal plane. Although a direct comparison was not conducted, we expect the balance performance may be higher than that of a robotic white cane system due to the SER characteristic of the system. Accordingly, future experiments will include direct comparisons between the RHC and conventional robotic navigation aids, especially for robotic white canes. Although robotic white cane systems have advantages in terms of compactness, portability, and ease of use in various outdoor environments [3], they do not provide a SER. Therefore, the RHC is expected to offer greater benefits in terms of gait balance improvement during robot-assisted guidance. Furthermore, to understand the level of trust and usability of the system, a further study will include a standardized survey (System Usability Scale, SUS).

The blind participant commented that he felt secure due to the system's intuitiveness from the fixed object-like characteristics during walking. Accordingly, the developed system may be intuitive since the robot directly guides the visually impaired along the path. Thus, users may easily adapt to the system. However, for practical use of the system, further improvements are necessary. Future research should address user-robot interactive control with a mobile manipulator platform on ramps or curbs, as well as level ground. For instance, the speed of the robot can be modulated based on the user's force response, using admittance control [17]. Furthermore, to provide SER, path planning with a smooth curve considering the user's gait balance presented in [32] can be used with our platform. Since the system is based on a mobile robot platform, it is currently suitable for application only on even ground, such as indoors. Additionally, since it has a high weight and is not portable, weight reduction is required for improving portability and suspended wheels may be necessary to overcome low bumps or uneven terrain for outdoor applications [33]. Since confidence and fear of falling negatively influence the gait capability during navigation of blind individuals [28], [34], for real-world applications, the system should include a sensor system capable of robust simultaneous localization and mapping techniques. Thus, since the system should ensure the safety of the user, a real-time obstacle sensing and avoidance planning technique is required during guidance [35]. A technique for distinguishing obstacles far from the user [36] can be combined with a prediction-based dynamic obstacle avoidance planning technique [35] to enhance user safety during guidance in complex real-world applications.

V. CONCLUSION

In this study, we evaluated the blinded gait during robot-assisted guidance with the provision of SER via the RHC. We conducted gait experiments with 20 sighted participants wearing blindfolds and one blind participant. Experimental results from the blindfolded sighted participants demonstrated that walking at a voluntary fast speed reduced gait stability (step width variability) and postural balance (mediolateral trunk tilt) compared to the preferred speed. However, the RHC allowed the sighted participants to walk more stably, especially at their voluntary fast speed. In addition, for the blind participant, the preferred speed improved with the use of the RHC. Moreover, gait balance (step width variability and mediolateral trunk tilt) was enhanced regardless of the speed. These results highlight the potential of the RHC to improve gait balance in blind individuals by providing SER during guidance. To gain a comprehensive understanding of the RHC's impact on the gait balance of the blind, future in-depth studies with larger numbers of blind individuals and various paths will be necessary.

ACKNOWLEDGMENT

The authors appreciate Yongseok Lee from Gwangju Segwang School for his advice from a visually impaired perspective during the design of the experimental protocol and system setup. *(Junyeong Lee and Hosu Lee are co-first authors.)*

REFERENCES

[1] D. Pascolini and S. P. Mariotti, "Global estimates of visual impairment: 2010," *Brit. J. Ophthalmology*, vol. 96, no. 5, pp. 614–618, May 2012.

[2] S. Gazzellini, M. L. Lispi, E. Castelli, A. Trombetti, S. Carniel, G. Vasco, A. Napolitano, and M. Petrarca, "The impact of vision on the dynamic characteristics of the gait: Strategies in children with blindness," *Exp. Brain Res.*, vol. 234, no. 9, pp. 2619–2627, Sep. 2016.

[3] P. Slade, A. Tambe, and M. J. Kochenderfer, "Multimodal sensing and intuitive steering assistance improve navigation and mobility for people with impaired vision," *Sci. Robot.*, vol. 6, no. 59, p. 6594, Oct. 2021.

[4] D. D. Clark-Carter, A. Heyes, and C. Howarth, "The efficiency and walking speed of visually impaired people," *Ergonomics*, vol. 29, no. 6, pp. 779–789, Jun. 1986.

[5] R. Dickstein and Y. Laufer, "Light touch and center of mass stability during treadmill locomotion," *Gait & posture*, vol. 20, no. 1, pp. 41–47, 2003.

[6] E. Kodesh, F. Falash, E. Sprecher, and R. Dickstein, "Light touch and medio-lateral postural stability during short distance gait," *Neurosci. Lett.*, vol. 584, pp. 378–381, Jan. 2015.

[7] M. Wuehr, R. Schniepp, C. Pradhan, J. Ilmberger, M. Strupp, T. Brandt, and K. Jahn, "Differential effects of absent visual feedback control on gait variability during different locomotion speeds," *Exp. Brain Res.*, vol. 224, no. 2, pp. 287–294, Jan. 2013.

[8] H. Lee, A. Eizad, G. Lee, M. R. Afzal, J. Yoon, M.-K. Oh, and J. Yoon, "Comparative study on overground gait of stroke survivors with a conventional cane and a haptic cane," *IEEE Trans. Neural Syst. Rehabil. Eng.*, vol. 29, pp. 2183–2192, 2021.

[9] K. Bingenheimer, J. J. Temprado, M. Harnagea, N. Bricot, P. Villani, and É. Berton, "Effects of a light touch on fixed or mobile supports on gait parameters in visually restricted young adults," *Neurosci. Lett.*, vol. 589, pp. 176–180, Mar. 2015.

[10] A. Forner-Cordero, V. D. Garcia, S. T. Rodrigues, and J. Duysens, "Obstacle crossing differences between blind and blindfolded subjects after haptic exploration," *J. Motor Behav.*, vol. 48, no. 5, pp. 468–478, Sep. 2016.

[11] R. K. Katzschmann, B. Araki, and D. Rus, "Safe local navigation for visually impaired users with a time-of-flight and haptic feedback device," *IEEE Trans. Neural Syst. Rehabil. Eng.*, vol. 26, no. 3, pp. 583–593, Mar. 2018.

[12] Z. Liao, J. V. S. Luces, and Y. Hirata, "Human navigation using phantom tactile sensation based vibrotactile feedback," *IEEE Robot. Autom. Lett.*, vol. 5, no. 4, pp. 5732–5739, Oct. 2020.

[13] C. Ye, S. Hong, X. Qian, and W. Wu, "Co-robotic cane: A new robotic navigation aid for the visually impaired," *IEEE Syst., Man, Cybern. Mag.*, vol. 2, no. 2, pp. 33–42, Apr. 2016.

[14] S. Kayukawa, T. Ishihara, H. Takagi, S. Morishima, and C. Asakawa, "BlindPilot: A robotic local navigation system that leads blind people to a landmark object," in *Proc. Extended Abstr. CHI Conf. Human Factors Comput. Syst.*, Apr. 2020, pp. 1–9.

[15] I. Shim and J. Yoon, "A robotic cane based on interactive technology," in *Proc. IEEE 28th Annu. Conf. Ind. Electron. Society*, vol. 3, Nov. 2002, pp. 2249–2254.

[16] V. Ranganeni, M. Sinclair, E. Ofek, A. Miller, J. Campbell, A. Kolobov, and E. Cutrell, "Exploring levels of control for a navigation assistant for blind travelers," in *Proc. ACM/IEEE Int. Conf. Hum.-Robot Interact.*, Mar. 2023, pp. 4–12.

[17] P. Balatti, I. Ozdamar, D. Sirintuna, L. Fortini, M. Leonori, J. M. Gandarias, and A. Ajoudani, "Robot-assisted navigation for visually impaired through adaptive impedance and path planning," in *Proc. IEEE Int. Conf. Robot. Autom. (ICRA)*, May 2024, pp. 2310–2316.

[18] C. F. Oliveira, E. R. Vieira, F. M. Machado Sousa, and J. P. Vilas-Boas, "Kinematic changes during prolonged fast-walking in old and young adults," *Frontiers Med.*, vol. 4, p. 207, Nov. 2017.

[19] J. Lee, H. Lee, A. Eizad, and J. Yoon, "A TENS based system for 2-dimensional balance biofeedback under muscle fatigue condition," *IEEE Access*, vol. 11, pp. 5724–5736, 2023.

[20] M. Andreetto, S. Divan, F. Ferrari, D. Fontanelli, L. Palopoli, and D. Prattichizzo, "Combining haptic and bang-bang braking actions for passive robotic Walker path following," *IEEE Trans. Haptics*, vol. 12, no. 4, pp. 542–553, Oct. 2019.

[21] A. Toumpa, A. Kouris, F. Dimeas, and N. Aspragathos, "Control of a line following robot based on FSM estimation," *IFAC-PapersOnLine*, vol. 51, no. 22, pp. 542–547, 2018.

[22] S. Suzuki, K. Hasegawa, Y. Makino, and H. Shinoda, "Haptic tracing of midair linear trajectories presented by ultrasound Bessel beams," in *Proc. Haptics, Sci.*, Jun. 2018, pp. 209–220.

[23] H. Lee, A. Eizad, J. Lee, and J. Yoon, "Development and evaluation of a gait assistance system based on haptic cane and active knee orthosis," in *Proc. Int. Conf. Robot. Autom. (ICRA)*, May 2022, pp. 5419–5425.

[24] O. Beauchet, C. Annweiler, Y. Lecordroch, G. Allali, V. Dubost, F. R. Herrmann, and R. W. Kressig, "Walking speed-related changes in stride time variability: Effects of decreased speed," *J. Neuroeng. Rehabil.*, vol. 6, no. 1, pp. 1–6, 2009.

[25] M. R. Afzal, S. Pyo, M.-K. Oh, Y. S. Park, and J. Yoon, "Evaluating the effects of delivering integrated kinesthetic and tactile cues to individuals with unilateral hemiparetic stroke during overground walking," *J. Neuroeng. Rehabil.*, vol. 15, no. 1, pp. 1–14, Dec. 2018.

[26] J. J. Jeka, R. D. Easton, B. L. Bentzen, and J. R. Lackner, "Haptic cues for orientation and postural control," *Perception Psychophysics*, vol. 58, no. 3, pp. 409–423, 1996.

[27] T. M. Owings and M. D. Grabiner, "Step width variability, but not step length variability or step time variability, discriminates gait of healthy young and older adults during treadmill locomotion," *J. Biomechanics*, vol. 37, no. 6, pp. 935–938, Jun. 2004.

[28] P. S. Haibach, J. Pritchett, and L. J. Lieberman, "Balance in adolescents with and without visual impairments," *Insight J.*, pp. 112–123, 2011.

[29] Y. Moon, D. A. Wajda, R. W. Motl, and J. J. Sosnoff, "Stride-time variability and fall risk in persons with multiple sclerosis," *Multiple Sclerosis Int.*, vol. 2015, pp. 1–7, 2015.

[30] P. A. Mensah, T. Agbezudor, A. Gyamfi, and R. Acquaye, "The white cane technique: A skill for reducing mobility dependence for Student with visual impairment," Research Square, Durham, NC, USA, Tech. Rep., 2023.

[31] T. Nakamura, "Quantitative analysis of gait in the visually impaired," *Disability Rehabil.*, vol. 19, no. 5, pp. 194–197, Jan. 1997.

[32] Q. Na, H. Zhou, H. Yuan, M. Gui, and H. Teng, "Improving walking path generation through biped constraint in indoor navigation system for visually impaired individuals," *IEEE Trans. Neural Syst. Rehabil. Eng.*, vol. 32, pp. 1221–1232, 2024.

[33] K. Alipour and S. A. A. Moosavian, "How to ensure stable motion of suspended wheeled mobile robots," *Ind. Robot, Int. J.*, vol. 38, no. 2, pp. 139–152, Mar. 2011.

[34] E. S. da Silva, G. Fischer, R. G. da Rosa, P. Schons, L. B. T. Teixeira, W. Hoogkamer, and L. A. Peyré-Tartaruga, "Gait and functionality of individuals with visual impairment who participate in sports," *Gait Posture*, vol. 62, pp. 355–358, May 2018.

[35] B. Guo, N. Guo, and Z. Cen, "Obstacle avoidance with dynamic avoidance risk region for mobile robots in dynamic environments," *IEEE Robot. Autom. Lett.*, vol. 7, no. 3, pp. 5850–5857, Jul. 2022.

[36] L. Gong, H. Chen, Y. Chen, T. Yao, C. Li, S. Zhao, and G. Han, "DPNet: Dynamic pooling network for accurate and efficient size-aware tiny object detection," *IEEE Internet Things J.*, vol. 12, no. 14, pp. 26387–26400, Jul. 2025.

JUNYEONG LEE received the B.S. degree in mechanical engineering from the School of Mechanical Engineering, Gwangju Institute of Science and Technology, Gwangju, South Korea, in 2022, where he is currently pursuing the Ph.D. degree with the Department of AI Convergence. In 2022, he joined the Department of AI Convergence, Gwangju Institute of Science and Technology. He was a Teaching Assistant with Gwangju Institute of Science and Technology, from 2022 to 2024. His current research interests include haptics, tactile feedback, rehabilitation, and human–robot interaction.

HOSU LEE received the B.S. and M.S. degrees from the School of Mechanical Engineering, Gyeongsang National University (GNU), Jinju, South Korea, in 2014 and 2016, respectively, the Ph.D. degree from GNU, in 2017, and the Ph.D. degree from the Department of Mechatronics, Gwangju Institute of Science and Technology (GIST), Gwangju, South Korea, in 2022. From 2016 to 2017, he was a Researcher with GNU. He was a Teaching Assistant of mechatronics and robotics with GIST, from 2019 to 2021. He was also a Postdoctoral Researcher with the Intelligent Medical Robotics Laboratory and the Cognition and Intelligence Laboratory, GIST. In 2023, he joined the Department of Control and Robot Engineering and the School of Aerospace Engineering, GNU, where he is currently an Assistant Professor. His current research interests include rehabilitation robotics, haptic feedback interfaces, cable-driven parallel robot (CDPR), and locomotion interface.

MINKYUNG KIM received the B.S. degree in human intelligence and robotics engineering from Sangmyung University, Cheonan, South Korea, in 2023, and the M.S. degree in intelligent robotics technology from the School of Integrated Technology, Gwangju Institute of Science and Technology (GIST), Gwangju, South Korea, in 2025. She is currently pursuing the Ph.D. degree with the Department of AI Convergence, GIST. Her research interests include human–robot interaction, gait stability, and haptics.

JIHO PARK received the B.S. and M.S. degrees from the School of Mechanical Engineering and the School of Integrated Technology, Gwangju Institute of Science and Technology, Gwangju, South Korea, in 2021 and 2023, respectively, where he is currently pursuing the Ph.D. degree with the Department of AI convergence. He was a Teaching Assistant of robotics with Gwangju Institute of Science and Technology, in 2023. His current research interests include mechatronics, medical robots, and mechanism synthesis.

JUNGWON YOON (Member, IEEE) received the Ph.D. degree in mechatronics from Gwangju Institute of Science and Technology (GIST), Gwangju, South Korea, in 2005. From 2001 to 2002, he was a Visiting Researcher with the Virtual Reality Laboratory, Rutgers University, Piscataway, NJ, USA, and a Visiting Fellow with the Functional and Applied Biomechanics Section, Department of Rehabilitation Medicine, Clinical Center, National Institutes of Health, Bethesda, MD, USA, from 2010 to 2011. He was also a Senior Researcher with the Electronics Telecommunication Research Institute (ETRI), Daejeon, South Korea. From 2005 to 2017, he was a Professor with the School of Mechanical and Aerospace Engineering, Gyeongsang National University, Jinju, South Korea. In 2017, he joined the Department of AI Convergence, GIST, where he is currently a Professor. Since 2019, he has been the Director of the Research Center for Nanorobotics in Brain (RCNB), GIST. He is also a principal project director in several large-scale research projects supported by South Korea Government in the themes of brain stimulation, drug delivery, and hyperthermia using nano robotics. He has authored or co-authored more than 200 peer-reviewed international journals and conference papers. His current research interests include magnetic particle imaging, bio-nano robot control, and rehabilitation robots. He was a Technical Editor of IEEE/ASME Transactions on Mechatronics and an Associate Editor of *Frontiers in Robotics and AI*.